LUND UNIVERSITY
Faculty of Science

Analysis and comparison of weather models for solar irradiance forecasts in Sweden

Bachelor thesis

Linus Falk

Supervisors:
Elna Heimdal Nilsson and Tomas Landelius

Swedish Meteorological and Hydrological Institute
Lund University, Department of Physics

April 2018

Abstract

Solar radiation is affected in a variety of different ways through the atmosphere and on its way down to the Earth's surface. Clouds are the main factor in this attenuation of solar radiation, but aerosols, ozone and other different gases have a significant impact too. Understanding these processes is fundamental to solar forecasting. However, the atmosphere is constantly changing, which makes forecasting weather a challenging task even with today's complex numerical weather prediction models.

In this study of solar irradiance, two different numerical weather models are analyzed: the global IFS-model and the regional ensemble prediction system MEPS. Both models include normal forecasts and ensemble forecasts. This analytical comparison was made in forecasts of up to 24 hours of three locations in Sweden over the time period of 2017-04-01 to 2017-06-30. The purpose was to see differences in the accuracy of the models, and also to see the influence of ensemble forecasts. Ensemble forecasts are used to better handle uncertainties in the weather and are more frequently used in today's weather prediction. Observation data collected from SMHI's radiation network was used as reference values in order to get forecasting errors.

A generally better result for the ensemble forecasts was identified. Some variations between the stations were also detected where especially the result from one of the three stations was different. That was a location far away from the other two indicating that topography and climatology can affect the precision of the weather models. The regional high-resolution MEPS-model had overall better solar irradiance forecasts during the analyzed time, but the model had a consistent negative bias. A consistent problem with the MEPS-model is probably that it predicts too much clouds which leads to less amount of solar irradiance in the forecasts.

Acknowledgement

First, I want to thank my supervisors Tomas Landelius and Elna Heimdal Nilsson for their encouragement, support and valuable tips during the entire Bachelor Thesis. A special thanks to Tomas who guided and helped me through many frustrating and technical issues besides topics of the thesis.

Secondly, I want to thank the department of Physics and every teacher I have had during my years at Lund University.

I am also grateful to all of my friends and family that supported me through this project, during both ups and downs.

Table of content

List of acronyms

ALADIN –	Aire Limitée Adaptation dynamique Développement InterNational
AROME –	Applications of Research to Operations at MEsoscale
DHI –	Direct Horizontal Irradiance
DNI –	Direct Normal Irradiance
ECMWF –	European Centre for Medium-range Weather Forecasts
EPS –	Ensemble Prediction System
GHI –	Global Horizontal Irradiance
HARMONIE–	HIRLAM-ALADIN Research for Mesoscale Operational Numerical weather prediction In Euromed
HIRLAM –	High Resolution Limited Area Model
IFS –	Integrated Forecast System
IFS-HRES –	IFS High-Resolution Ensemble System
MEPS –	Metcoop Ensemble Prediction System
MetCoOp –	Meteorological Cooperation for Operational weather
NSC –	National Supercomputer Centre
NWP –	Numerical Weather Prediction
PV –	Photovoltaic
RRTM –	Rapid Radiative Transfer Model
SMHI –	Swedish Meteorological and Hydrological Institute
TSI –	Total Solar Irradiance

1. Introduction

The understanding in interactions of solar radiation with the Earth's atmosphere form a basis of solar forecasting. Solar irradiance at surface of the Earth is a highly irregular parameter mainly due to Earth's rotation and cloud cover but aerosols and different gases in the atmosphere have a significant impact too.

Weather models are complicated mathematical models based on physical laws and equations, and by knowing current atmospheric condition they can help us predicting how the weather will be within a short future. In this project, two particular weather models will be in focus. HARMONIE-AROME is a non-hydrostatic regional weather model developed by several European meteorological institutes and IFS is a hydrostatic global weather model controlled by European center for meso-scale weather forecasts (ECMWF).

Ensemble forecasts are a way to handle uncertainties in weather forecasting. Running a weather model several times, each run with slightly different initial values gives a better understanding in how the atmosphere will be in the future. Many weather models are therefore using ensemble forecasts to improve weather forecasts. MEPS is an ensemble predication system controlled by Sweden, Norway and Finland based on the model HARMONIE-AROME.

The massive growth of solar power over the last decades have led to an increasing demand of accurate solar radiation forecasts. Solar forecasting is a major area of interest in the field of solar power due to the variability and uncertainty of solar irradiance. Energy companies are interested in both the short-term forecasts and the long-term forecasts to make the solar power industry more effective. By knowing how much solar power that will be produced, energy operators can balance and regulate with other power sources so that total supply (production) and demand (consumption) correspond, in order to have a robust and flexible power grid. Many studies have been made on solar forecasting but there is a lack of knowledge for Sweden and the Nordic countries. Solar power is very likely going to have a significant role in light of the goal to have a 100% renewable electricity system 2040 set by the Swedish government. Knowledge of the variability and uncertainty of solar irradiance in both time and space is going to be valuable to manage and plan the renewable electrical system for Sweden in the future.

The aim of the present study is to get a deeper understanding in solar forecasting for Sweden by comparing and analyzing forecast data from one global and one regional weather model. SMHI will provide real station measurements as a reference, and the model comparison will be between IFS and MEPS.

This thesis attempts to show the differences between two weather models in forecasts of solar irradiance in up to 24 hours. The impact of ensemble forecasts in the models and the spread if the ensemble members will be analyzed.

Research questions:

- Which one of the two numerical weather models is the most accurate for solar irradiance forecasts in Sweden?
- Can the forecasts be improved with ensemble forecasts?
- How good and distributed are the ensemble members?

2. Background

2.1 Radiation and atmospheric effects

To understand solar forecasting, it is beneficial to have wide background knowledge about radiation and properties of the Earth's atmosphere that affect solar radiation.

2.1.1 Electromagnetic radiation

The sun constantly emits electromagnetic radiation in all directions and only a fraction of the total radiation strikes Earth. In fact, all objects no matter its size with a temperature above absolute zero radiates energy across a range of wavelengths in the electromagnetic spectrum (Ahrens 2008). Objects with a high temperature emits more total radiation each second, which is described in Stefan-Boltzmann law:

$$E = \sigma \cdot T^4 [\mathrm{W/m^2}] \tag{1}$$

where $\sigma = 5.67 \cdot 10^{-8}\ \mathrm{W} \cdot \mathrm{m}^{-2} \cdot \mathrm{K}^{-4}$ is Stefan Boltzmann constant, E is the maximum rate of radiation emitted by each square meter of the object and T is the surface temperature of the object. This formula is applied for black bodies, which means objects that are emitting the maximum radiation for its temperature.

Electromagnetic radiation travels as waves with different wavelengths primarily depending on the temperature of the emitting object. Surface of the sun is approximately 5800 K and the Earth only about 290 K (Ahrens 2008). By using Wien's displacement law, a law describing the relationship between the temperature of the object and the wavelength of the emission maximum (λ_{max}), the wavelengths of the electromagnetic radiation from these two celestial bodies can be determined.

$$\lambda_{max} = \frac{2.89777 \cdot 10^{-3}\ \mathrm{m \cdot K}}{T} \qquad [\mathrm{m}] \tag{2}$$

Accordingly, with Wien's constant known, most of the Earth's emitted radiation has a wavelength of 5-25 µm with its emission maximum at 10 µm. Figure 1 displays the Solar spectrum where 97% of the solar radiation is in the wavelength spectrum of 290-3000 nm (Kleissl, 2015). This is the reason why radiation from the Sun is often called shortwave radiation, while the Earth's emitting radiation is called longwave radiation (Ahrens 2008). Shortwave radiation is hence mostly in the spectrum of visible and infrared light with some part of the ultraviolet radiation.

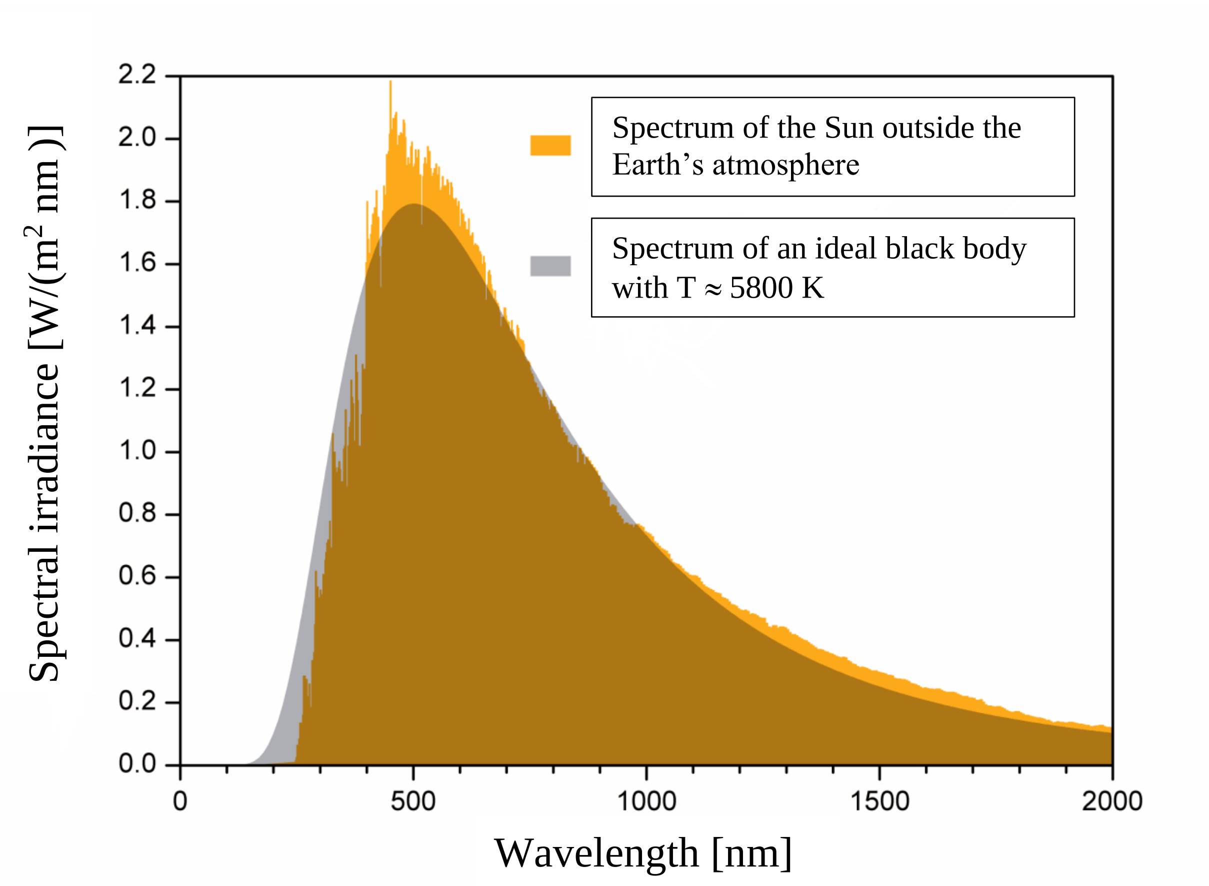

Figure 1*: The solar spectrum with spectral irradiance as a function of wavelength. Grey shows a 5800 K ideal black body with and orange shows spectrum of the Sun outside the Earth's atmosphere.*

The amount of shortwave radiation reaching a surface area is often called solar irradiance and is measured as power per unit area (W/m^2). The total residual solar radiation reaching the top of Earth's atmosphere is called Total Solar Irradiance (TSI) or the Solar constant, measured perpendicular to the incoming solar radiation with a value of 1361± 0,5 W/m^2 (Kopp, 2011). This value corresponds to the area under the graph in figure 1. Small fluctuations of the TSI occur due to Earth's elliptical orbit around the Sun.

Variations of solar irradiance happen in both time and place at surface of the Earth. Annual variations occur due to Earth's tilted axis with respect to the Earth's orbit around the sun and this tilt is approximate 23.45°. Diurnal variations of solar irradiance appear due to the rotation of Earth and give different solar zenith angles (SZA) during the day. Solar irradiance at the Earth is divided into diffuse horizontal irradiance (DHI), direct normal irradiance (DNI) and global horizontal irradiance (GHI). GHI is defined as the total amount of shortwave radiation received from above by a surface per unit area horizontal to the ground. DNI is instead measured on a planar surface normal to the Sun, and that allows DNI to exceed GHI during sunny days. The three solar irradiance components are related in the following mathematical way and an example of variations during a week for DNI and GHI is shown in figure 2.

$$GHI = \cos(SZA) \cdot DNI + DHI \qquad [W/m^2] \qquad (3)$$

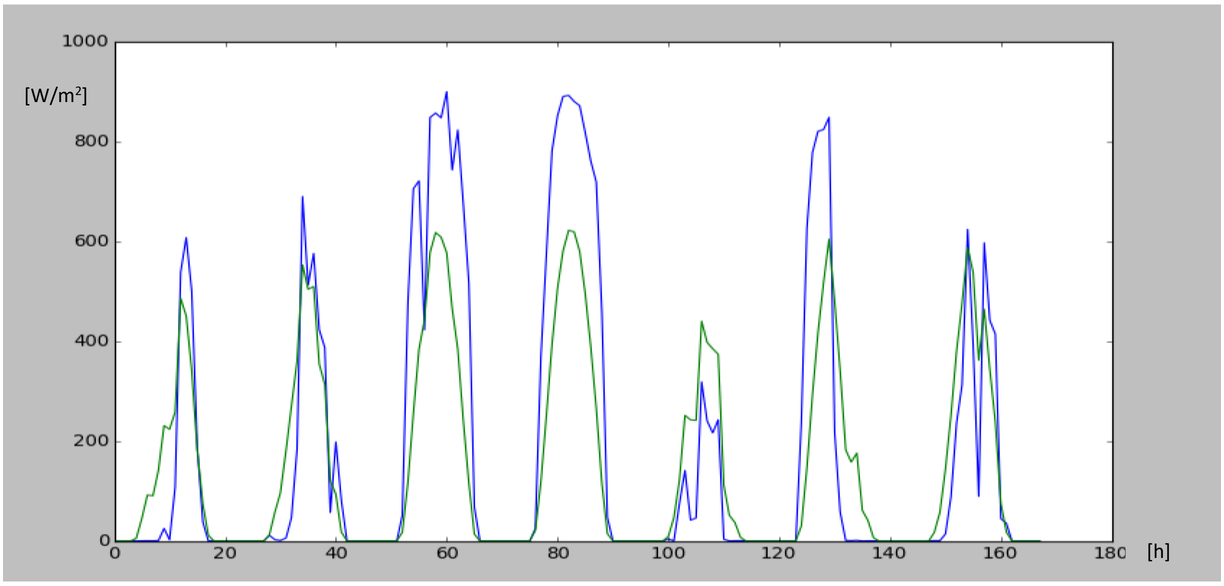

Figure 2: *Example of GHI (green) and DNI (blue) variations during a week (168 hours) at surface of the Earth.*

2.1.2 Atmospheric interactions with solar radiation

Solar radiation is affected in various ways through the atmosphere. Absorption, reflection and scattering are central physical processes in the atmospheric attenuation of solar radiation (Welch and Koch, 1980). Clouds is the main influence on solar irradiance at the Earth's surface but Kleissl (2015) clarifies that even during a cloudless day solar radiation is affected through the atmosphere. Aerosols, water vapor, ozone and other small components of the atmosphere reduce the amount of shortwave radiation reaching the surface of the Earth. Some shortwave radiation is directly reflected at the top of the atmosphere or blocked in the upper part of the atmosphere.

Absorption of electromagnetic radiation is an important process in the Earth's atmosphere. During absorption, the energy is converted to another form where the radiation is no longer present at the same wavelength after impact. For gaseous absorption, important molecules in the atmosphere are O_2, O_3, H_2O, CO_2, CH_4 and N_2O.
Molecules absorb the electromagnetic radiation by changing their vibrational, rotational or electrical state. Electrical transitions occur mainly in the UV-region of the electromagnetic spectrum with nitrogen, oxygen and ozone as absorbers, while rotational and vibrational transitions occur in the infrared region with H_2O and CO_2 as efficient absorbers. Oxygen, Methane, carbon dioxide and N_2O are relatively even distributed in the atmosphere while ozone and H_2O concentrations depend more on time and location.

Scattering of electromagnetic radiation occur in a number of different ways, depending on the size of the particle and the wavelength of the incoming radiation. To begin with, Rayleigh scattering happens when the diameter of the particle is less than 1/10 the wavelength of the incoming radiation. This type of scattering is strongly wavelength dependent with short wavelengths of the radiation being scattered more, and that is e.g. the reason that the sky appears blue. Rayleigh scattering is a simple but good approximation for ozone (O_3), nitrogen dioxide (NO_2) and other small particles and molecules in the atmosphere (H.A Fricker, 2009). Mie scattering on the other hand is a more exact solution used when particles (Aerosols) approximate at the same size as the wavelength of the incoming radiation are present. This occurs mainly in the lower part of the atmosphere where larger particles such as dust, pollution and water droplets are more abundant. An important difference between Rayleigh scattering and Mie scattering is the scattering angles shown in figure 3.

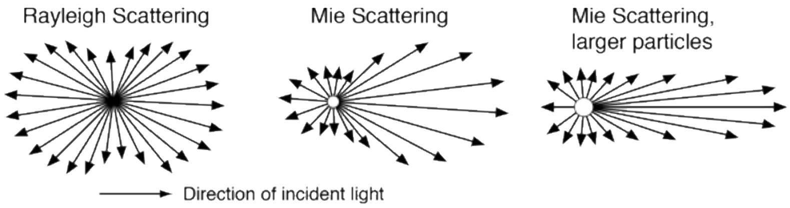

Figure 3*: The electromagnetic radiation scatters in different angles depending on the size of the particle.*

Clouds have different albedos[1] depending on their thickness, but it is on average 60 percent (Ahrens 2008). Clouds have as mentioned a major effect on how much solar radiation that reaches the Earth's surface. Welch and Koch (1980) further explains that factors such as cloud type, cloud top height, cloud thickness, liquid water content and drop size distribution affects how much the solar radiation transmits and reflects. Mentioned scattering and absorption effects therefore give different cloud albedos.

The size of the cloud droplets is important to what kind of physical process that will occur on impact with electromagnetic radiation. In interactions with cloud droplets, shortwave radiation can be scattered in all directions as mentioned earlier. However, larger cloud droplets absorb a larger amount of the incoming shortwave radiation. This is happening in clouds that produce large cloud droplets and raindrops and is the reason these clouds appear darker.

An overview of the atmospheric interactions with solar radiation can be shown in the shortwave portion of the Earth's energy budget (left part of figure 4). The portion of shortwave radiation reflected by clouds and the atmosphere (23%) in figure 4 is actually both scattered and reflected effects. The values in figure 4 are global averages and would change if we look at different locations or times due to the changing weather.

[1] The percentage of reflected light compared to incoming light striking the surface is called albedo.

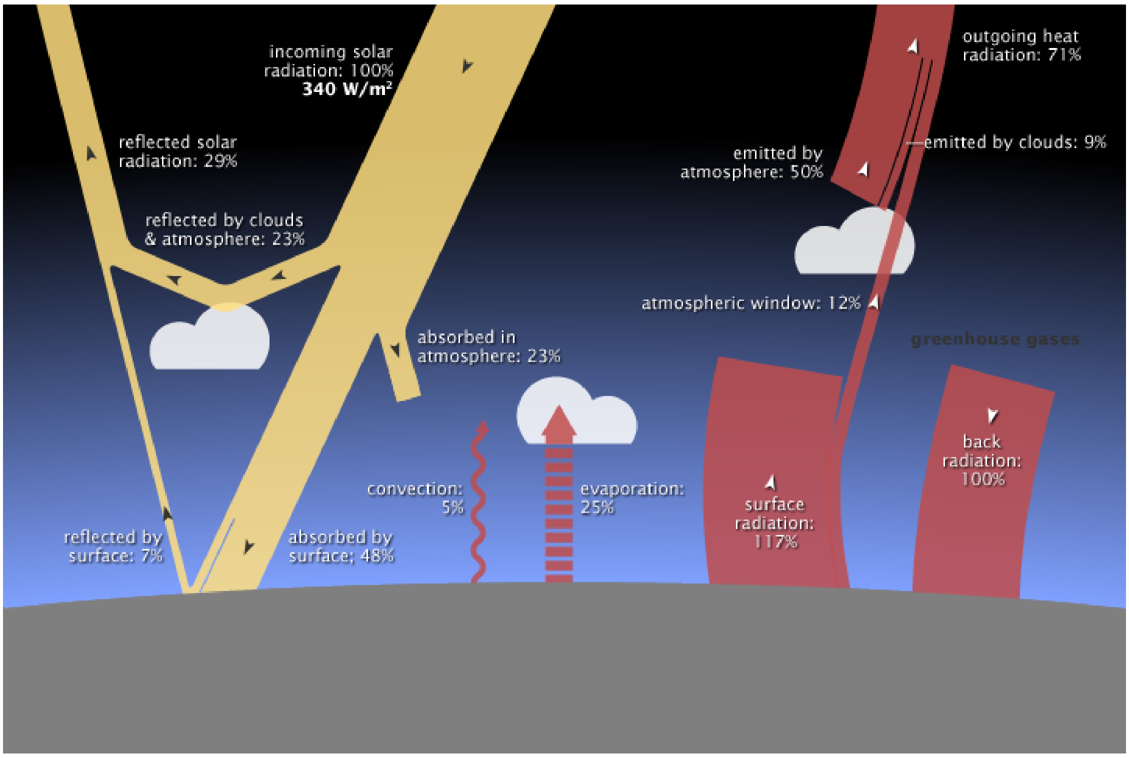

***Figure 4**: Earth's energy budget. To the left is the shortwave portion of the energy budget. 340 W/m^2 is the mean solar irradiance for the whole Earth (TSI/4) and corresponds to 100% incoming shortwave radiation (Lindsey, 2009).*

2.2 Weather forecasting

Significant changes of solar irradiance occur over time periods of many minutes to hours due to the rotation of Earth, but these variations are fairly easy to predict. Changes in cloud cover on the other hand are more irregular and uncertain and can happen in seconds. To be able to predict solar irradiance, we need weather forecasts.

2.2.1 Numerical weather prediction

The difficulty of forecasting weather is a physical and mathematical problem and can be solved by numerical weather prediction (NWP). NWP-models have become a crucial part of weather forecasting and they are mathematical models that use the laws of physics and the current weather situation to predict the future state of the atmosphere and oceans.

The current weather situation can be measured by meteorological observations such as satellites, weather balloons, radars, weather stations, ships and aircrafts. Almost all of the weather phenomena appear in the lowest part of the atmosphere called the troposphere. The observations however are not distributed homogenously in space and time. By using observation data and the latest weather forecast data, a more complete atmosphere can be described in a process called data-assimilation. This gives the initial values of our NWP models.

NWP-models use equations concerning atmospheric dynamics and these equations need to be solved numerically and not analytically. The equations are mostly non-linear partial differential equations describing atmospheric flow, and to solve these equations (in numerical weather models) supercomputers with high level computing performance are needed.
The primitive equations form the mathematical basis in NWP-models, including the ideal gas law and conservation laws of energy, mass and momentum. In this section, they will in short be described but derivation and further explanation can be found in other literature. However, many more physical laws and equations are included in NWP-models e.g. equations describing moist air. The primitive equations relate the variables pressure (*p*), temperature (*T*), zonal velocity (*u*), meridional velocity (*v*) and vertical velocity (*w*) and density (ρ).

Using Newton second law on a box of air where the acceleration is the sum of all forces affecting the air parcel gives the momentum equation (here in vector form).

$$\frac{\mathbf{F}}{m} = \boldsymbol{a} = \frac{D\mathbf{U}(u,v,w)}{Dt} = -\frac{1}{\rho}\nabla p - 2\mathbf{\Omega} \times \mathbf{U} + \mathbf{g} + \mathbf{F}_{\text{friction}} \tag{4}$$

Involved forces are the pressure gradient force, the Coriolis force, gravitational force and friction where $\mathbf{\Omega}$ is Earth's rotation rate, $\mathbf{g}$ is the gravitational force and $\mathbf{F}_{\text{friction}}$ is the friction.

Below shows the x- and y-component of the momentum equation where $f = 2\Omega\sin(\varphi)$ is the Coriolis parameter.

$$\frac{Du}{Dt} = fv - \frac{1}{\rho}\frac{\partial p}{\partial x} \tag{5}$$

$$\frac{Dv}{Dt} = -fv - \frac{1}{\rho}\frac{\partial p}{\partial y} \tag{6}$$

The vertical component of the momentum equation can be approximated and expressed as the hydrostatic balance equation with no vertical acceleration. This is only valid if the horizontal scale is much larger than the vertical scale and the approximation can therefore not be done in high-resolution weather models.

$$\frac{\partial p}{\partial z} = -\rho g \tag{7}$$

Conservation of energy in the atmosphere is explained by the first law of thermodynamics. This formula explains how the air parcel's temperature changes:

$$c_p\frac{DT}{Dt} - \alpha\frac{Dp}{Dt} = J \tag{8}$$

where c_p is the specific heat of constant pressure, $\alpha = \frac{1}{\rho}$ is the specific volume, and J is the rate of heating.

The continuity equation explains the conservation of mass for a fluid. In meteorology, the atmosphere is described as a continuous medium and the continuity equation explains the relationship between convergence/divergence and vertical motion.

$$\left(\frac{\partial u}{\partial x} + \frac{\partial v}{\partial y}\right)_p + \frac{\partial \omega}{\partial p} = 0 \qquad (9)$$

The final primitive equation is the ideal gas law, describing the equation of state for an ideal gas.

$$p = \rho R_s T \qquad (10)$$

In this version of the ideal gas law R_s is the specific gas constant defined as R/M. M is the molar mass and R is the gas constant with a value of 8.3144598 $\mathrm{J \cdot mol^{-1} \cdot K^{-1}}$. However, all the primitive equations can be expressed in other forms e.g. in different coordinate systems.

In fluid dynamics, instead of looking at individual molecules the atmosphere is treated as continuous and divided into small volumes and this assumption is called the continuum approximation. It allows atmospheric variables such as temperature pressure and density to be represented as smooth and continuous functions taking on unique values in space and time. Discretization is a mathematical process to approximate and solve a continuous problem into a discrete, and this is done to solve the differential equations in NWP. There are different solution methods the weather models use to solve the equations and predict the future state of the atmosphere. A model can even use different methods for different spatial dimensions. The simplest discretization method is the finite difference method, mostly used by regional models. Another similar method is the spectral method, mainly used by global models. Operational weather forecast models use both the spectral method and the finite difference method for horizontal discretization.

According to Holton and Hakim (2012), parametrization in weather models is one of the most controversial and difficult area in predicting the weather with NWP. Weather models have different spatial resolutions (grid spacing), but some meteorological phenomena are active on smaller scales than the spatial resolution and are therefore too complex for the models to interpret. Figure 5 shows the most important physical processes that often are parametrized in NWP-models. Convection, clouds and radiative flux are examples of small-scale processes (scale of less than 1 km) that are described by other large-scale weather variables such as wind speed, temperature and pressure. Holton and Hakim (2012) further explain that convection is perhaps the most important process to parameterize. One example of parametrization connected to solar radiation can be a few hundred meters thick cloud layer, actually too small for the numerical weather model to resolve even though the cloud has a huge impact on solar irradiance. By parametrization the cloud can be interpret into the model.

***Figure 5**: Small-scale weather processes that are commonly parameterized in NWP-models. (https://scienceandtheworld.wordpress.com/2013/06/19/wading-into-the-fire-episode-9-parameterization-schemes/)*

2.2.2 Ensemble forecasts

Weather models are not perfect, mainly due to limitations in computer power, model errors and uncertainty in the initial conditions. The atmosphere is of chaotic nature and small errors in a deterministic numerical forecast will grow rapidly with time. Ensemble forecasts are probabilistic forecasts and often used in NWP to handle uncertainties in the forecast models. It means that the computer runs the model several times with marginally different initial condition where each individually forecast is called an ensemble member. This gives a number of different final forecasts and together they are called an ensemble forecast or probability forecast. A mean of all the outcomes can subsequently be used and the spread of the ensemble members gives the prediction uncertainty. In ensemble prediction systems (EPS), the model physics is also often slightly perturbed and sometimes several weather models can be combined in one ensemble forecast (WMO, 2012). A control member is an ensemble member without any perturbation.

To evaluate the ensemble spread, a diagnostic tool called rank histogram (or Talagrand diagram) can be used. Hamill (2001) describes that a rank histogram is a good tool to determine the reliability of the ensemble forecast and to spot errors in its mean and in the spread of the ensemble members. The structure of rank histograms differs from ordinary histograms and can be explained in a few steps.

All the ensemble members are first listed by its forecasted value for a chosen variable, and the difference between two adjacent values forms a bin in the rank histogram. An observation value now gets placed in the right bin depending on its value, and this is repeated for the observation value a chosen number of days. Left part of figure 6 is an example of ensemble members listed by its forecasted value (in this case temperature). The observation value appears to be between the second and third listed value and therefore comes in the third bin. The right part of figure 6 shows an example of a complete rank-histogram with 20 ensemble members.

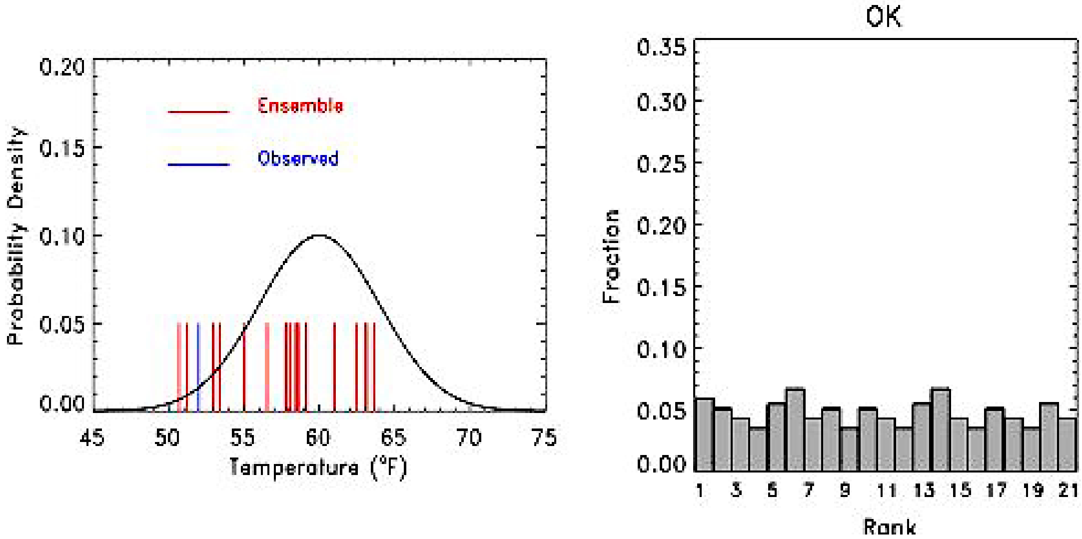

Figure 6*: An example of how a rank-histogram is created. Left part is ensemble members listed by its temperature at a given time. The observation value clearly comes third and consequently the third bin in the rank-histogram can be partly filled. This procedure is repeated until a complete rank-histogram is formed like the one to the right.*

With n total ensemble members, the number of bins will consequently be n+1. The bins are accordingly created by the forecast data and then filled with observation data. A large sample of data is necessary when it comes to rank histograms in order to achieve a trustworthy result. A resulting flat rank-histogram indicates that the ensemble members have been distributed in a good way. A sloped rank histogram will have a consistent bias in the forecast data (Houtekamer, 1998; Hamill, 2001).

2.2.3 Cloud-initialization and the Spin-up problem

It is widely known that good cloud and humidity predictions plays a fundamental role in solar radiation forecasts. However, clouds are difficult for the weather models to handle because of the non-linear and discontinuous cloud microphysical processes. Clouds are normally not included in the NWP data-assimilation, while variables such as temperature and humidity are included and may therefore not be in physical balance with the cloud field. This effect is called the spin-up effect, and the time it takes for the model to achieve physical balance between the variables is called spin-up time. A good initial balanced cloud field with other variables is important in short solar irradiance forecasts, and it makes the forecast valuable most of the first six hours (H. Gaston et al., 2013).

2.2.4 Forecasting solar irradiance and solar power

Solar forecasting is fundamental in the large-scale production of electricity through solar power. By using the photovoltaic (PV) effect, energy from the sunlight can be directly converted to electricity and that is happening in a PV solar cell. In this energy conversion, normal PV solar cells can only use the high-intensity energy photons in the visible part of the electromagnetic spectrum.

Solar power is at this point considered as the fastest-growing energy industry in the world (Solangi 2011). Technologies are getting better, and material costs are decreasing but energy companies are confronting two key issues: variability and uncertainty. Large changes in solar power, so-called ramp-events needs to be predicted with high accuracy because they have a huge influence in the balance of supply and demand (Kleissl 2013). The Swedish solar cell market is at this point in a period of very strong growth. The number of installed solar cells is increasing rapidly towards the goal to have a 100% renewable electricity system in Sweden by 2040.

Solar power production clearly depends on meteorological conditions and is therefore difficult to predict. A future for Sweden with a large portion of irregular solar power with high demand response will be a changeover from today's power generation. By making solar power forecasts, conditions are created for the electrical system operators to be more flexible and effective in their planning. Predictions of solar irradiance [W/m^2] can easily be converted to electric power predictions [W] by knowing the area of the solar cell. Only small losses are happening in the conversion process (Kleissl, 2013).

There are different approaches in short-term forecasting of solar irradiance (Perez, 2013). A comprehensive explanation of NWP-models has already been made (chapter 2.2.1), where forecasts of several days in advance can be valid. Another useful approach to predict cloud-motion is satellite remote sensing and ground-based sky measurements. This method, often imbedded in weather models, is useful in forecast of a few hours. The last approach is statistical time-series models that uses solar irradiance data in forecast of minutes up to a few hours.

Despite the advanced NWP weather models with massive computer capability, forecasting solar irradiance is a challenging task. Sources of error in forecasted solar irradiance can be many, both regarding clouds and during non-cloudy conditions. Aerosol representation, ozone representation and water-vapor absorption are common clear-sky errors in NWP-models (Kleissl, 2013). NWP-models also in general have a tendency to predict too many thick clouds and less thin clouds. A possible reason for this is too coarse vertical grid spacing in the models, making thin clouds tough to resolve.

2.2.4 IFS-model

ECMWF is one of the most prominent institution for global medium-range NWP and was developed 1975 by several European countries. The integrated forecast system (IFS) is the

Earth-system weather model developed at ECMWF. There are two different versions within the atmospheric IFS: the high-resolution model IFS-HRES and the ensemble forecast model IFS-ENS. IFS-HRES is the high-resolution deterministic forecast model with two model-runs per day and a horizontal resolution of 9 km. The dynamic core of IFS is hydrostatic. The deterministic IFS is a spectral model and uses a semi-implicit semi-Lagrangian discretization.

IFS use the Rapid Radiative Transfer Model (RRTM), which is a part of the fully McRad radiation scheme. RRTM considers water vapor, ozone, methane, carbon dioxide, aerosols, nitrous oxide and various chlorofluorocarbons (IFS documentation Cy43r1, 2017). Cloud-radiation interactions are treated with the Monte Carlo Independent Column Approximation method (McICA). A new radiation scheme called ECRAD was installed summer 2017 with some slight improvements from the previous version of IFS. However, during this analysis and time period the old McRaD scheme was still operational.

Since 1992, ECMWF has also operated with ensemble forecasts. IFS-ENS is the ensemble prediction system of ECMWF and has 51 ensemble members, each with a horizontal resolution of 18 km. The control member has the same resolution as the other members. Further details about the IFS-models can be found on the ECMWF website.

2.2.5 HARMONIE-AROME and MEPS

Another NWP model is the non-hydrostatic HARMONIE-AROME (HIRLAM ALADIN Regional Meso-scale Operational NWP in Europe-Application of Research to Operations at Mesoscale) used for short-range operational weather forecasts mostly in northern Europe.
The model was developed from a meteorological cooperation between the north-western European research group HIRLAM and the central European research group ALADIN and is based on the French model AROME (Applications of Research to Operations at Mesoscale).

The HARMONIE-AROME configuration is a spectral model and uses the same non-hydrostatic dynamical core as AROME-France. HARMONIE-AROME is based on the fully compressible Euler equations, and just like IFS the dynamics is built on a two-time level semi-implicit and semi-Lagrangian discretization.

The development from AROME to HARMONIE-AROME led to improvements in the model's physical parametrization (e.g. in the physical description of clouds) but new and small updates of HARMONIE-AROME is happening all the time. HARMONIE-AROME uses the same shortwave parametrization scheme as ECMWF. Shallow convection needs to be parametrized but there is no parametrization of deep convection due to the 2.5 km horizontal resolution. A similar radiation scheme used by IFS is also used by HARMONIE-AROME.

A cooperation between Norway, Sweden, and Finland called MetCoOP has been running the HARMONIE-AROME (version harmonie-40h1.1) since 2014, and 2016 they included ensemble forecasts. The ensemble prediction system of MetCoOP is shortened MEPS and contain one control member and nine perturbed members. A horizontal resolution of 2.5 km is possible for MEPS due to a relative small forecast domain (figure 7) compared to many other weather models. MEPS uses 65 vertical levels of the atmosphere and boundary and initial conditions are taken from the deterministic IFS-HRES. In Sweden, the National Supercomputer Centre (NSC) in Linköping runs all the numerical weather calculations concerning HARMONIE-AROME. Post processing of MEPS in Sweden is handled by SMHI (Andrae, 2017).

***Figure 7**: The forecast domain of MEPS which contain Sweden, Norway and Finland. This is the same domain as in HARMONIE-AROME.*

The ensemble members have applied perturbations to surface variables in MEPS since June 2017. Perturbations are applied on boundary and initial values by using the SLAF-method (Scaled lagging average forecasting), which differ from the method in IFS-ENS. Normal perturbations are though applied in the same way as for IFS-ENS.

To briefly summarize the last two sections about weather models, the main differences between the involved models in this thesis are horizontal and vertical resolution, number of ensemble members and perturbation technique of the ensemble members.

***Table 1**: Configuration details of the models. ctl=control member, mbrs=ensemble members.*

Model	**IFS-HRES**	**IFS-ENS**	**MEPS(ctl/mbrs)**
Horizontal resolution	9 km	18 km	2.5 km
Vertical levels	137	91	65
Forecast members	1	51	10
Forecast horizon	~10 days	~15 days	~ 48h/ 66h
Dynamics	Hydrostatic	Hydrostatic	Non-hydrostatic
Forecast update rate	12 h	12 h	6 h

3. Methodology

3.1 Data

Swedish meteorological and hydrological institute (SMHI) provided observation data from their radiation network in Sweden. An upgrade of the radiation system was done 2007. The focus in this project was at the three advanced stations in Kiruna, Norrköping and Visby shown in figure 8, that measured both DNI and GHI. DNI was measured with an instrument called pyrheliometer (of model Kipp & Zonen CH1) that automatically follows movement of the sun. GHI on the other hand was measured with pyranometers (of model Kipp & Zonen CM21). These two different types of instruments have been accurately calibrated, and both measures wavelength of 200-4000 nm. The observation data covers the time period of 2017-04-01 to 2017-06-30 with measurements collected every hour.

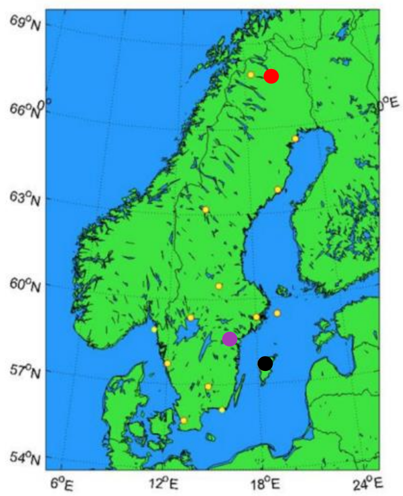

***Figure 8**: Meteorological radiation network of SMHI. Kiruna (red), Norrköping (purple) and Visby (black) are the advanced stations measuring GHI and DNI (SMHI).*

The data processing and analysis was made in the Ipython software connected to the National Supercomputer Centre in Linköping (NSC) through Secure Shell (SSH). High storage of forecast data was available from both MEPS and IFS-models. Interpolated forecast-data to the three locations in Kiruna, Norrkoping and Visby was obtainable from both IFS-model and MEPS with DNI and GHI as analyzed parameters. The data-sets had an hourly time-step for both models.

The data from MEPS had all 10 ensemble members included, with available forecasts every day from 00, 06, 12 and 18 UTC. This dataset from MEPS had some missed and incorrect values that later had to be adjusted. The data from IFS (Cy43r1 version) consisted of the high resolution deterministic forecast IFS-HRES and the ensemble forecast IFS-ENS with its 51 members. Since the IFS-models are running twice a day, forecast data was available at 00 and 12 UTC each day.

3.2 Working process

Firstly, all the meteorological data was structured and organized. High amount of meteorological data for many parameters was available but only GHI and DNI was used in this analysis. The analysis was divided into two main parts: model comparison and ensemble forecasts evaluation.

In the first analysis, the global weather model IFS and the high-resolution model MEPS were analyzed in forecasts of 0-24 hours with forecasts starting at 00 UTC. Deterministic forecast and ensemble forecast of both weather models were scrutinized for the three locations with GHI and DNI as analyzed meteorological parameters. Observation data from stations at SMHI was used as reference in order to get bias and standard deviation. Bias values were generated with observation data subtracted from forecast data in order to create a positive bias when a model predicts too much irradiance. Mean values of all the ensemble members for each weather model were produced. MEPS forecast from 06 UTC was added for comparison with the model run at 00 UTC. The reason for this was to detect possible spin-up effect or other start-up errors in the model but also to see if the forecast from 06 UTC had better accuracy for any range of forecast. Only model run starting at 00 UTC was used for IFS.

In the second analysis, the ensemble forecasts IFS-ENS and MEPS were scrutinized with rank histograms to get information about the spread and reliability. DNI-values were adjusted with a factor since a clear-sky systematic error was detected. This error of too little forecasted solar irradiance during clear-sky conditions was determined by looking at the error for the control member with each weather model during clear sky conditions. A mean scaled value from several clear days were created, 1.240 for MEPS and 1.188 for IFS. The same scaled “factor value” was used for all three stations. Consequently, two rank-histograms for each EPS were obtained.

4. Results

4.1 Analysis and comparison of IFS and MEPS

Plots will now be presented in forecasts of up to 24 hours mainly with forecasts from the very start of the day at 00 UTC. MEPS can produce a new forecast six hours later (as distinct from IFS) and that forecast will also be presented in the plots. The purpose of this analysis is to distinguish differences between the models but also within the models (for ensemble mean, control member etc.). Plots with MEPS and IFS apart, and with all respectively ensemble members can be seen in appendix. Before the results are presented, it is beneficial to know some things:

- The **standard deviation** is the square root of the average of the squared deviations from the mean.
- The mean of the forecasting errors is called **bias** and is used to describe systematic deviations of the forecasts.
- Figure 9 below shows the mean observation solar irradiance, and this can be used to put the upcoming forecasting errors in perspective.

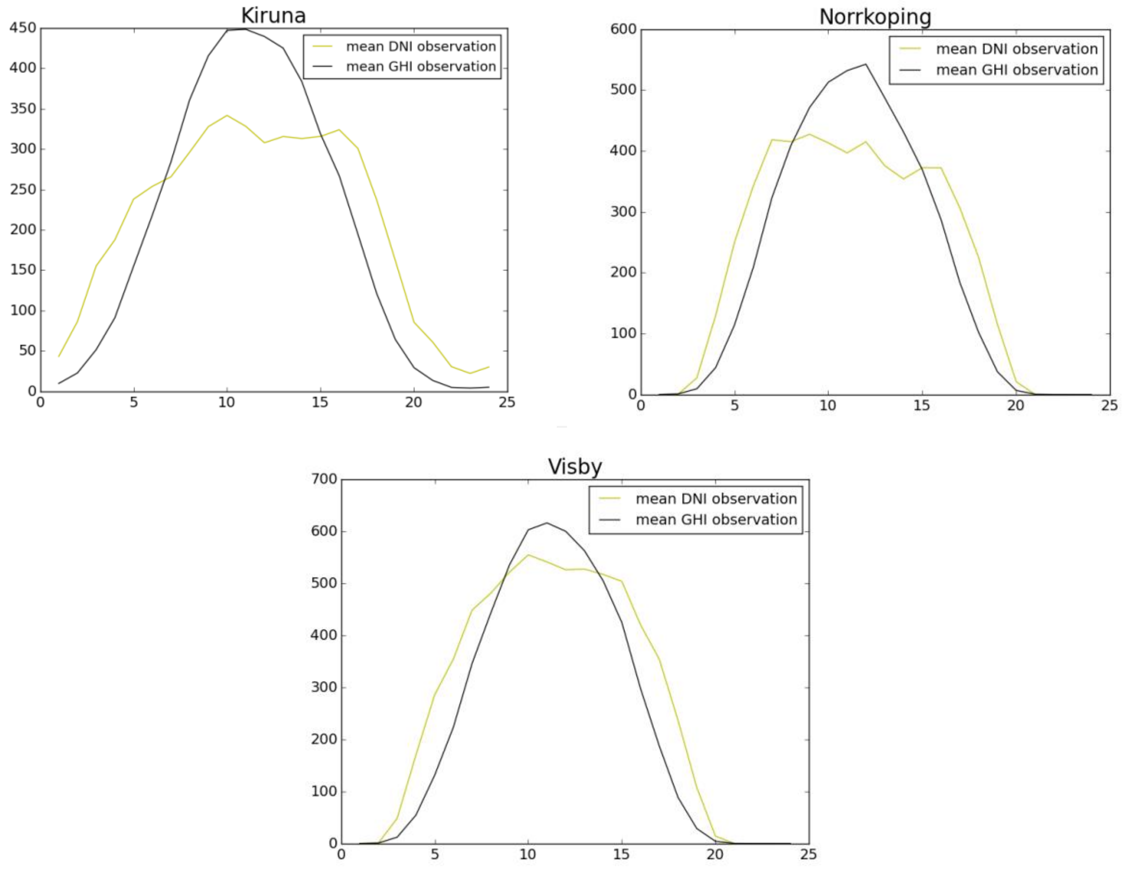

Figure 9: *The mean observation values of DNI and GHI during April-June 2017 for the three stations. Displays the solar irradiance [W/m^2] as a function of time [h].*

Global horizontal irradiance (GHI):

By plotting the mean standard deviation of the forecast errors between forecast data and observation, accuracy of the models can be compared.

In figure 10 (**a-c**), GHI forecasts done at 00 UTC for every hour the next coming 24 hours is shown. Model run at 06 UTC is added for MEPS. From the figure, ensemble mean is definitely more accurate than the control member in both ensemble forecasts. In Norrkoping (**b**) and Visby (**c**) MEPS had better prognoses than the global IFS-model during the given time period. Kiruna shows a bit different result with IFS slightly more accurate than MEPS. The 06 UTC model run for MEPS gives no distinct forecast improvement compared to the 00 UTC run, except some small improvements at forecast for the afternoon. Overall, the forecasting errors in Kiruna are fairly huge compared to the actual observation values in figure 9.

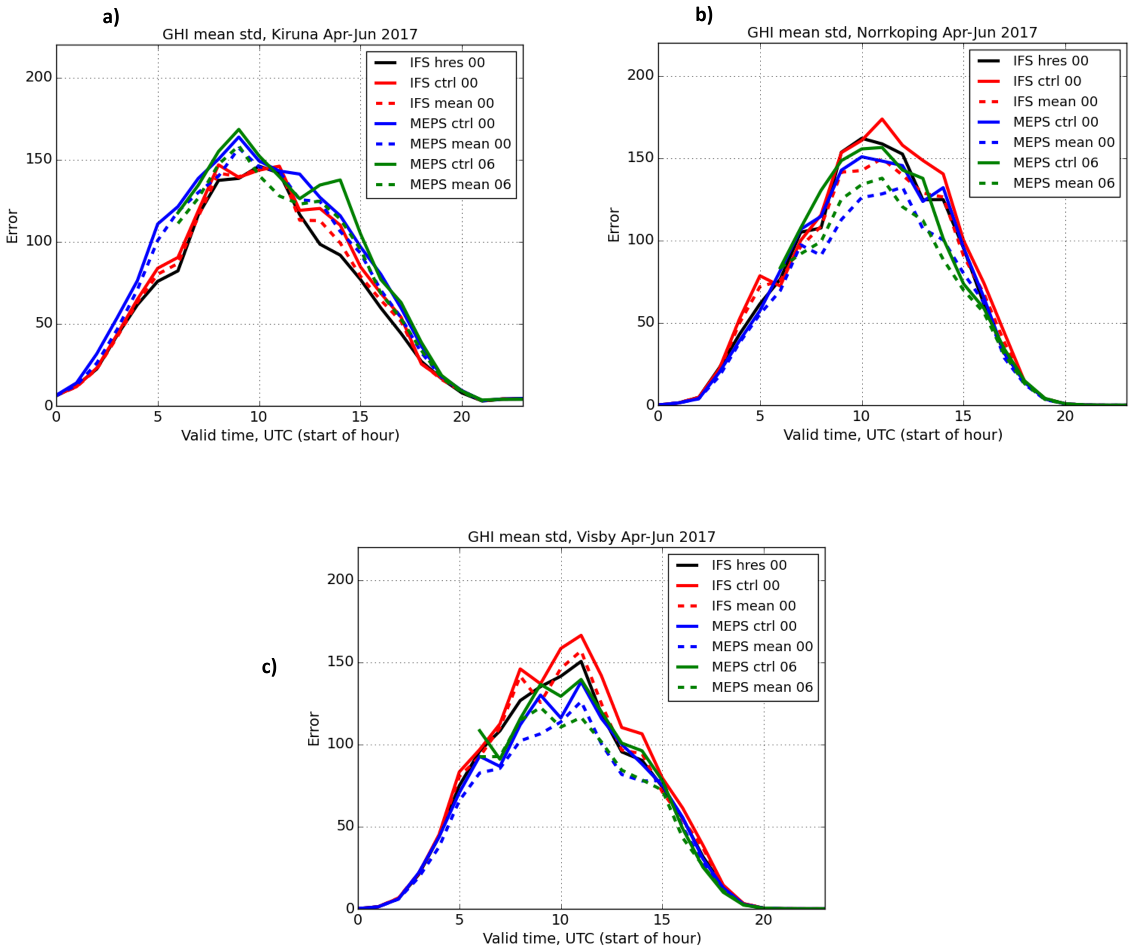

***Figure 10**: Mean GHI forecast errors [W/m^2] for Kiruna (**a**), Norrkoping (**b**) and Visby (**c**).*

By studying forecast errors of GHI even further, bias of the models is shown in figure 11 (**a-c**). With a negative bias, MEPS did a underprediction of solar irradiance for all location (**a-c**) but it is extra clear in Kiruna (**a**). The IFS-model also shows a slight overall underprediction of solar irradiance but not that significantly compared to MEPS. MEPS ensemble mean forecast run at 06 UTC has a really negative bias the first hours.

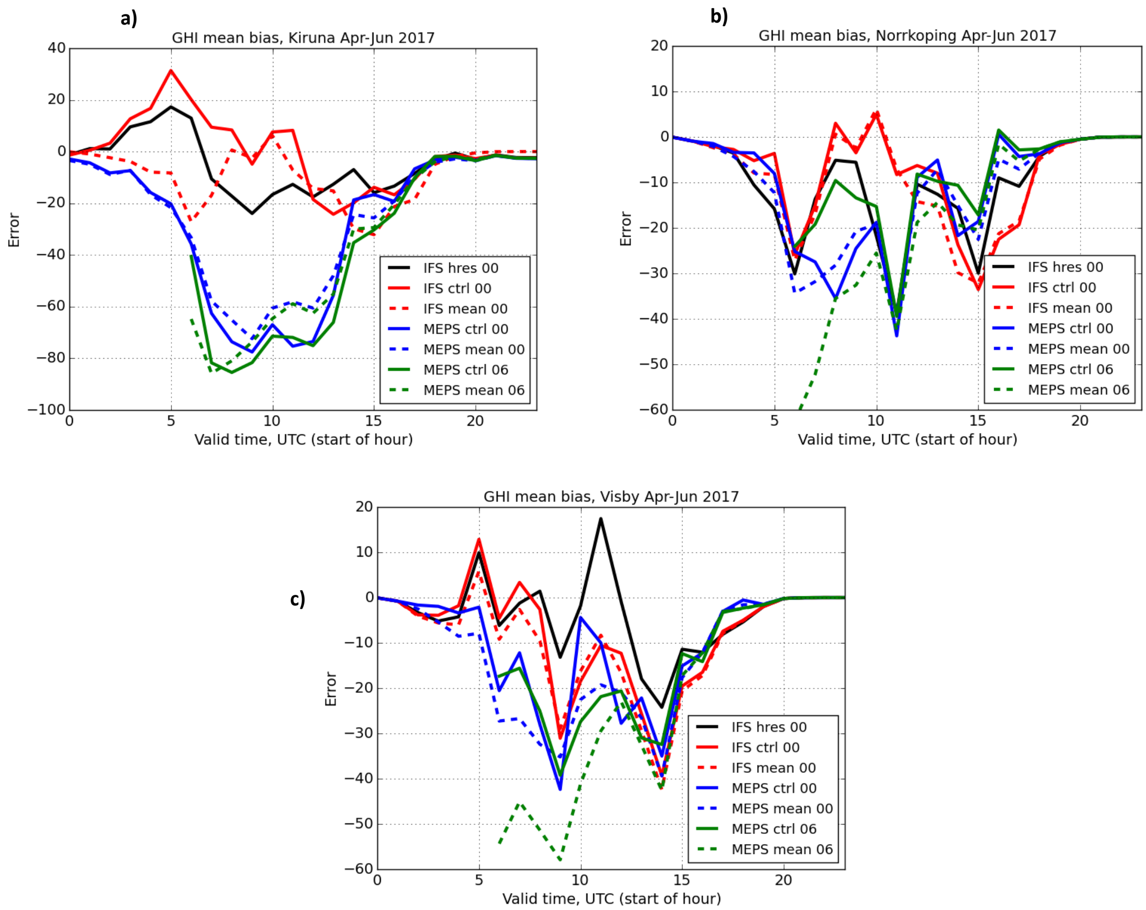

***Figure 11**: Mean forecast bias of GHI [W/m^2] for Kiruna (**a**), Norrkoping (**b**) and Visby (**c**).*

Direct normal irradiance (DNI):

The same procedure for DNI gives three new plots with model forecast comparison (figure 12 **a-c**). Similar results compared to GHI are displayed for the standard deviation of DNI forecast errors with generally better results for MEPS compared to the IFS-model (**b-c**). The result for Kiruna (**a**) shows the opposite, with more accurate DNI forecasts for IFS (same as with GHI).

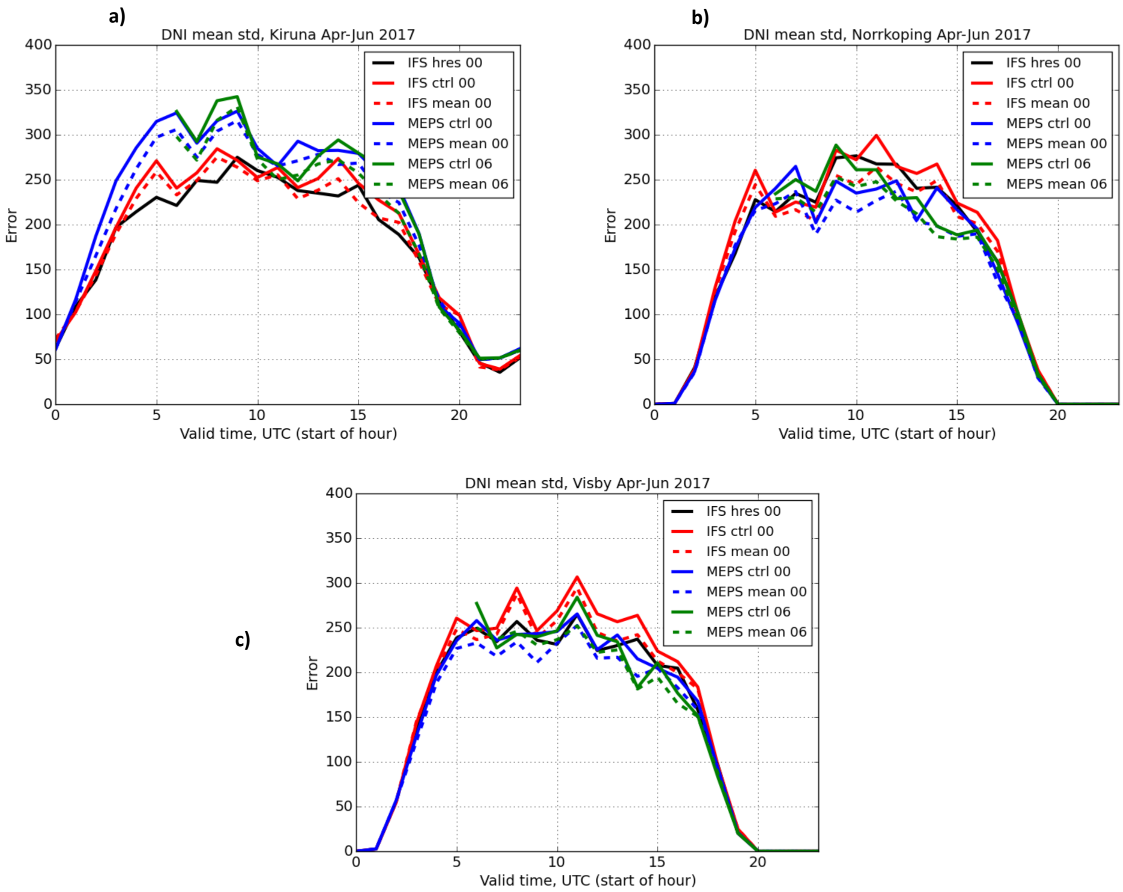

***Figure 12**: Mean DNI forecast errors [W/m^2] for Kiruna (**a**), Norrkoping (**b**) and Visby (**c**).*

A small positive bias for IFS and a more distinct negative bias for MEPS can be detected in figure 13 (**a-c**). The 06 UTC model run for MEPS gives no improvement compared to the run at 00 UTC. The forecast from 06 UTC have a far more distinct negative bias for the early day forecasts than the forecast from 00 UTC shows.

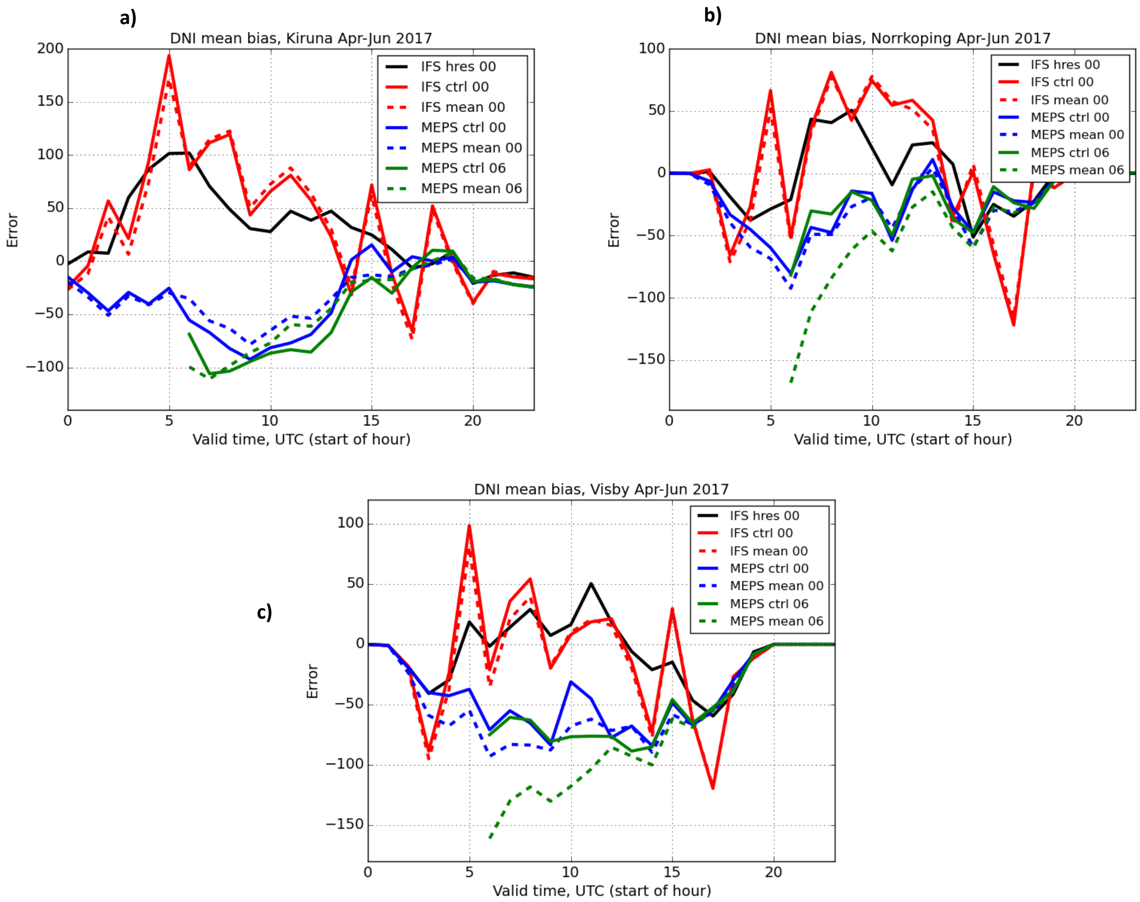

Figure 13*: Mean forecast bias of DNI [W/m^2] for Kiruna (****a****), Norrkoping (****b****) and Visby (****c****).*

4.2 Reliability and spread of the ensemble forecasts

Rank-histograms are here used to evaluate the spread of the ensembles, without considering the forecast accuracy right now. The detected systematic clear-sky error for DNI was therefore first removed by scaling forecast values with a factor (1.240 for MEPS and 1.188 for IFS). These scaled values were determined by taking the mean forecasting errors of the control-members during clear days. Figure 14 shows the resulting rank-histograms for the spread of the 51 members in IFS-ENS. Both rank-histogram for DNI (left) and GHI (right) have a U-shaped form with much observation data outside the spread of the members.

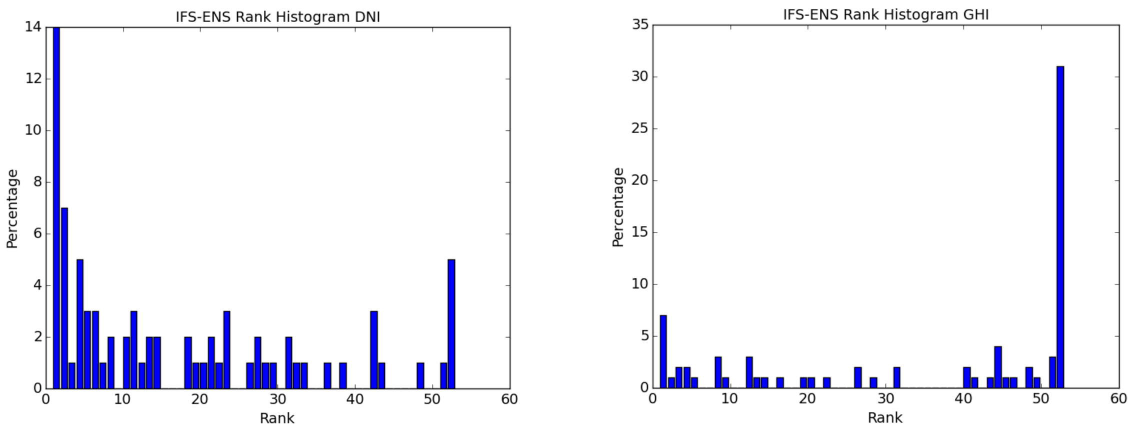

Figure 14: *Rank histogram of the ensemble prediction system IFS-ENS. DNI (left) and GHI (right) as parameters.*

Rank-histograms were also made for the ensemble prediction system MEPS and its 10 members. The result in figure 14 displays one rank-histogram for DNI (left) and one for GHI (right). The rank-histogram for DNI appears to be much flatter than GHI for MEPS and the two for IFS-ENS.

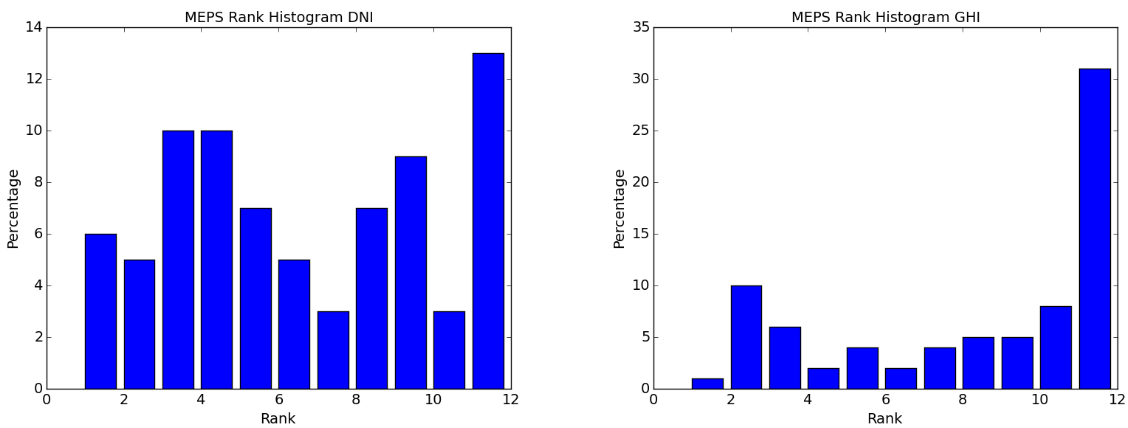

Figure 15: *Rank histogram of the ensemble prediction system MEPS. DNI (left) and GHI (right) as parameters.*

5. Discussion and conclusion

Two different numerical weather models were scrutinized in this analysis. The aim was to: see which one of the models that had best prediction of solar irradiance (DNI and GHI), detect any biases of solar irradiance in the models, and determine the accuracy and spread of the ensemble forecasts.

Firstly, the ensemble system MEPS (based on the high-resolution model HARMONIE-AROME) in general showed better solar irradiance forecasts compared to the IFS-model. The exception was for the location in Kiruna that showed the opposite. Some differences between the stations were thus detected where specially the result from Kiruna was different. Kiruna is a city far north in Sweden, far away from the other two cities (see figure 8), indicating that differences in topography and climatology can affect the accuracy of the weather models. No exact explanation of this difference between locations was found.

Taking ensemble mean from all of the ensemble members gave the best forecast result within MEPS, but IFS-HRES was overall slightly better than the ensemble-mean of IFS-ENS. This can be due to the difference in spatial resolution between IFS-HRES (9 km) and IFS (18 km).

MEPS seems to have a negative bias when it comes to predicting the solar irradiance in Sweden. The model is most likely overpredicting clouds in general, which leads to a negative bias of solar irradiance.

The impact of the added forecast from 06 UTC gave no distinct improvements compared to the original forecast from 00 UTC. Only the control member gave a decent result. Maybe some missing coding error or measurement error could have been done here due to the extreme differences. The spin-up effect can most likely not be the whole explanation since only the bias was totally inaccurate. An explanation can be that perturbations in the ensemble members give forecasts of too much clouds in the beginning of the forecasts. The forecasts from 00 UTC obviously show no visible spin-up effect or other early-hour errors since the first hours of the day have close to zero solar irradiance.

The evaluation of ensembles by rank histograms gave some interesting results. The IFS-model with its large amount of ensemble members probably needs a bigger spread at the initial time since the rank histogram showed a clear “U-shape” with observation data mostly in the two outer bins. MEPS appeared to have a slightly better spread of the ensemble members considering the flatter rank histogram in figure 15. It is possible that the sample data in this rank-histogram analysis was too small. With a time period of 91 days and only three stations, the result is sensitive to errors.

References

Ahrens, C.D. (2008). *Meteorology today: An Introduction to Weather, Climate and the Environment.* 11th edition. 39-57

Andrae, U. (2017). *The MetCoOp EPS.* Available at: https://www.smhi.se/polopoly_fs/1.127225!/K%C3%B6rnich_MEPS_poster_ECMWF_201709.pdf [Accessed 1 Mars 2018]

Bengtsson, L et al. (2017). *The HARMONIE-AROME model configuration in the ALADIN-HIRLAM NWP System*

Driesenaar, T. (2009). *General description of the HARMONIE-AROME model.* Available at: http://hirlam.org/index.php?option=com_content&view=article&id=65:general- [Accessed 1 Mars 2018]

ECMWF. (2017) *IFS documentation CY43R1, Part III*
ECMWF. (2017) *IFS documentation CY43R1, Part IV*
ECMWF. (2017) *IFS documentation CY43R1, Part V*
Available at:
https://www.ecmwf.int/search/elibrary/IFS?secondary_title=%22IFS%20Documentation%20CY43R1%22 [Accessed 1 Mars 2018]

Fricker, H.A *Lecture on Propagation, Dispersion and scattering.*
Available at: http://topex.ucsd.edu/rs/Lec07.pdf [Accessed 1 Mars 2018]

Gaston, M., Landelius, T., Schroedter-Homscheidt, M. and Bergeman, C. (2013). *Direct Normal Irradiance Nowcasting methods for optimized operation of concentrating solar technologies.* DNIcast

Hamill, T.M. (2001) *Interpretation of Rank Histograms for Verifying Ensemble Forecasts*

Holton, J and Hakim, G. (2012). *An Introduction to Dynamic Meteorology*. Volume 88. Fifth edition. 474-475

Houtekamer, P (1998). *ABC of ensemble forecasting.* Available at: http://collaboration.cmc.ec.gc.ca/cmc/cmoi/product_guide/docs/lib/ens_en.pdf [Accessed 1 Mars 2018]

Inman, R.H. Pedro., H.T.C and Coimbra, C.F.M. (2013). *Solar forecasting methods for renewable energy integration*. Progress in Energy and Combustion Science. Vol 39. 535-576

Kleissl, J. (2013). *Solar Energy Forecasting and Resource Assessment*.
Chapter 1,5,6,12

Kopp, G and Lean, J.L. (2011). *A new, lower value of the total solar irradiance: Evidence and climate significance*

Lindsey, R. (2009). *Climate and Earth's Energy budget.* NASA earth observatory.
Available at: https://earthobservatory.nasa.gov/Features/EnergyBalance/page1.php [Accessed 1 Mars 2018]

Liou, K.N. (1980). *An introduction to Atmospheric radiation*, *Volume 84.* Second edition.
Chapter 3

Solangi, K.H. (2011). *A review on global solar energy policy*. Vol 15. 2149-2163

Young and Freedman. (2011) *University physics with Modern Physics.* 13th edition. Volume 1

Young and Freedman. (2011) *University physics with Modern Physics.* 13th edition. Volume 2

WMO. (2012). *Guidelines on Ensemble Prediction Systems and Forecasting.* Available at:
http://www.wmo.int/pages/prog/www/Documents/1091_en.pdf [Accessed 1 Mars 2018]

Appendix

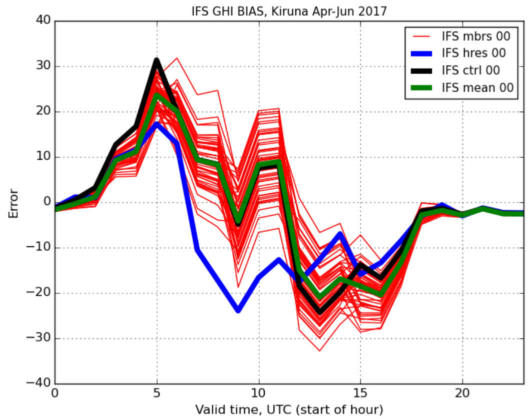
IFS GHI BIAS, Kiruna Apr-Jun 2017
IFS mbrs 00
IFS hres 00
IFS ctrl 00
IFS mean 00
Error
Valid time, UTC (start of hour)

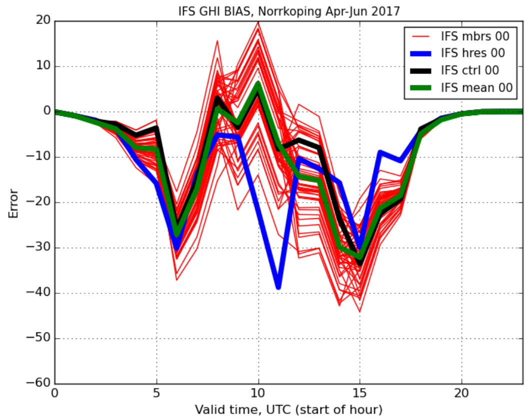
IFS GHI BIAS, Norrkoping Apr-Jun 2017
IFS mbrs 00
IFS hres 00
IFS ctrl 00
IFS mean 00
Error
Valid time, UTC (start of hour)

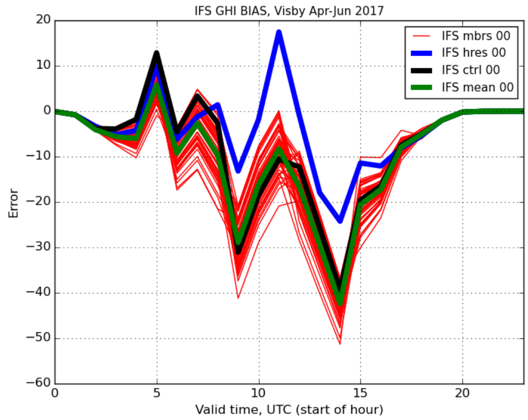
IFS GHI BIAS, Visby Apr-Jun 2017
IFS mbrs 00
IFS hres 00
IFS ctrl 00
IFS mean 00
Error
Valid time, UTC (start of hour)

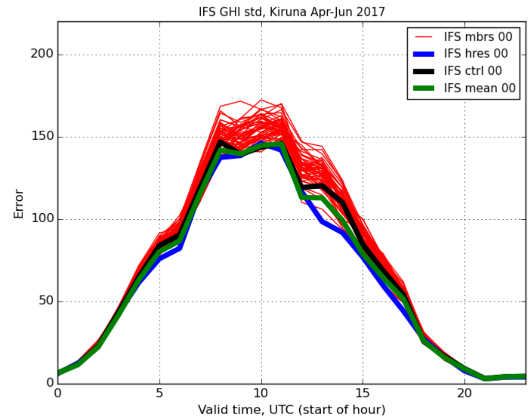
IFS GHI std, Kiruna Apr-Jun 2017
IFS mbrs 00
IFS hres 00
IFS ctrl 00
IFS mean 00
Error
Valid time, UTC (start of hour)

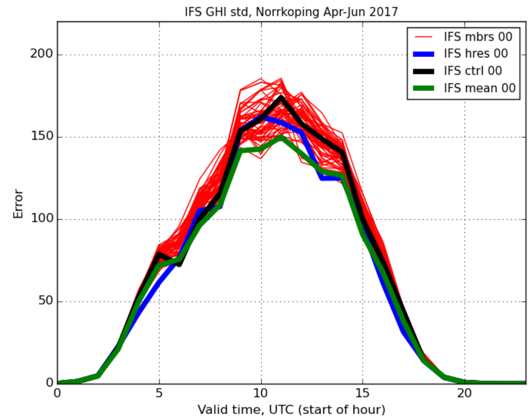
IFS GHI std, Norrkoping Apr-Jun 2017
IFS mbrs 00
IFS hres 00
IFS ctrl 00
IFS mean 00
Error
Valid time, UTC (start of hour)

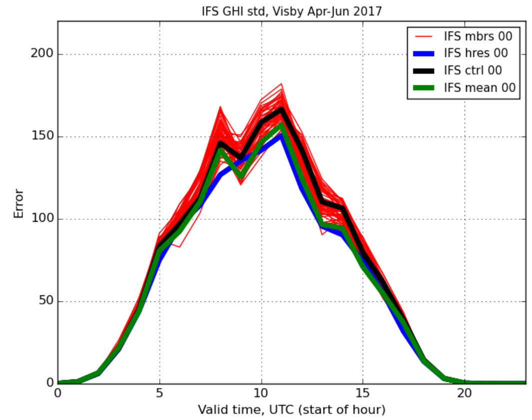
IFS GHI std, Visby Apr-Jun 2017
IFS mbrs 00
IFS hres 00
IFS ctrl 00
IFS mean 00
Error
Valid time, UTC (start of hour)

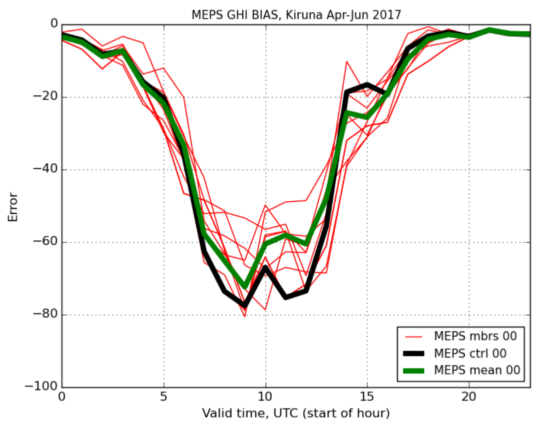
MEPS GHI BIAS, Kiruna Apr-Jun 2017
MEPS mbrs 00
MEPS ctrl 00
MEPS mean 00
Error
Valid time, UTC (start of hour)

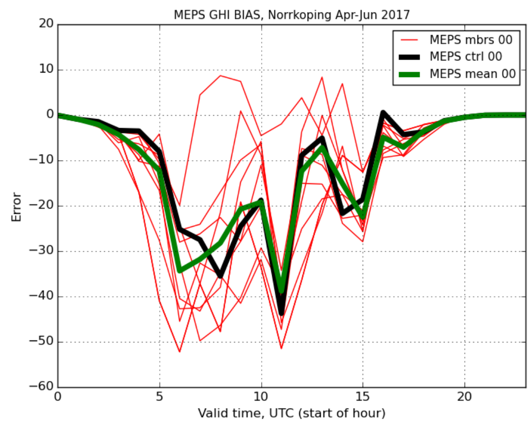
MEPS GHI BIAS, Norrkoping Apr-Jun 2017
MEPS mbrs 00
MEPS ctrl 00
MEPS mean 00
Error
Valid time, UTC (start of hour)

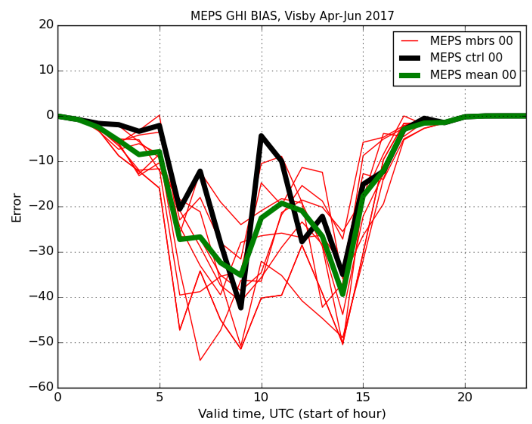
MEPS GHI BIAS, Visby Apr-Jun 2017
MEPS mbrs 00
MEPS ctrl 00
MEPS mean 00
Error
Valid time, UTC (start of hour)

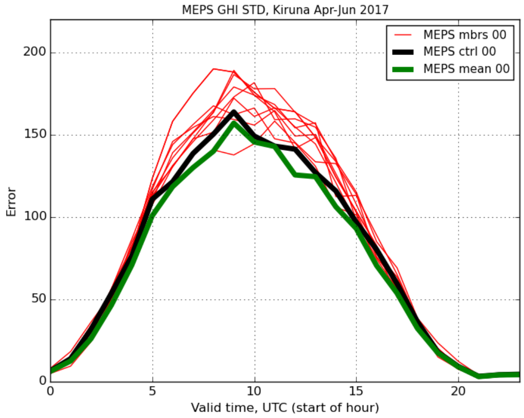
MEPS GHI STD, Kiruna Apr-Jun 2017
MEPS mbrs 00
MEPS ctrl 00
MEPS mean 00
Error
Valid time, UTC (start of hour)
0
50
100
150
200
0
5
10
15
20

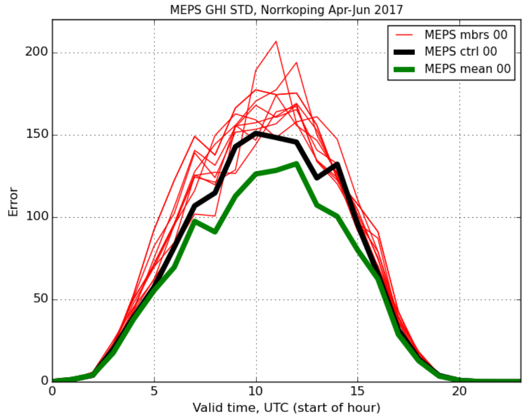
MEPS GHI STD, Norrkoping Apr-Jun 2017
MEPS mbrs 00
MEPS ctrl 00
MEPS mean 00
Error
Valid time, UTC (start of hour)
0
50
100
150
200
0
5
10
15
20

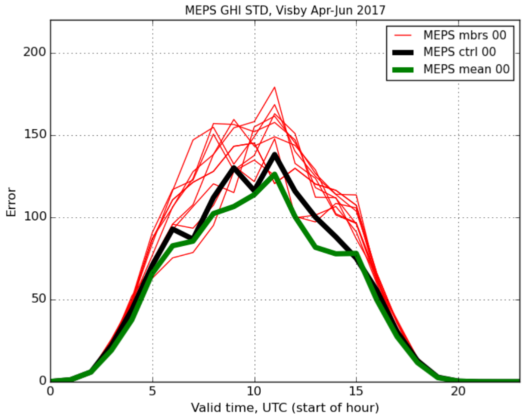
MEPS GHI STD, Visby Apr-Jun 2017
MEPS mbrs 00
MEPS ctrl 00
MEPS mean 00
Error
Valid time, UTC (start of hour)
0
50
100
150
200
0
5
10
15
20